FACTORS OF SAFETY FOR RICHARDSON EXTRAPOLATION FOR INDUSTRIAL APPLICATIONS

by

Tao Xing and Fred Stern

Sponsored by
The Office of Naval Research
Grant N00014-01-1-0073
N00014-06-1-0420

IIHR Technical Report No. 466

IIHR—Hydroscience & Engineering
College of Engineering
The University of Iowa
Iowa City, Iowa 52242-1585 USA

September 2008

TABLE OF CONTENTS

List of Tables

List of Figures

List of Nomenclature

C_k = correction factor

ε = solution change

Fr = Froude number

FS = factors of safety

p = order of accuracy

R = solution ratio

r = refinement ratio

S = solution

U = uncertainty; velocity

y^+ = wall coordinate ($= U_\tau y / \nu$)

$\delta^*_{RE_{k_1}}$ = error

ν = kinematic viscosity

Subscripts

1 = first grid point away from the wall

1,2,3 = fine, medium, and coarse grids, respectively

C = corrected

G = grid

k = the k^{th} parameter

RE = Richardson Extrapolation

th = theoretical

τ = frictional

Abstract

Improved factors of safety for quantitative estimates for grid and time convergence uncertainties for CFD solutions are proposed for situations when Richardson extrapolation estimated order of accuracy p_k is larger than the theoretical order of accuracy $p_{k_{th}}$ and correction factor 1<C_k<2. The improved uncertainty estimates are shown to provide more reasonable intervals of uncertainty for $p_k > p_{k_{th}}$ (1<C_k<2).

I. INTRODUCTION

Current procedures for quantitative estimates for grid and time convergence uncertainties for CFD solutions are based on first-order Richardson extrapolation (RE) error estimates with factors of safety (*FS*) used for expanded uncertainty estimates. Roache [1,2] proposed the grid-convergence index (GCI) with *FS*=1.25 for systematic grid-triplet studies using RE estimate for order of accuracy p_k ($k=G$ for grid, $k=T$ for time, and $k=P$ for similar parameters) and *FS*=3 for 2-grid sensitivity studies using theoretical estimate for order of accuracy $p_{k_{th}}$. The GCI is widely used and recommended by ASME [3] and AIAA [4]. The authors and colleagues proposed a correction factor (C_k) method [5,6] with linearly increasing *FS* vs. distance from the asymptotic range (AR) $C_k = (r_k^{p_k} - 1)/(r_k^{p_{kth}} - 1)$, which was based on analytical benchmarks that approach the AR with $p_k < p_{k_{th}}$. *FS* was reflected for $p_k > p_{k_{th}}$. *FS* using C_k is smaller than *FS*=1.25 for solutions very close to the AR, whereas *FS* using C_k is much larger than *FS*=1.25 for solutions far from the AR, which is the typical situation for industrial applications. C_k has the "common-sense" advantage compared to GCI in providing a quantitative metric to determine proximity of the solutions to the AR and approximately accounts for the effects of higher-order RE terms. The C_k method has been used in ship hydrodynamics CFD workshops.

A deficiency of both GCI and C_k methods is that for $p_k > p_{k_{th}}$ the uncertainty estimates are unreasonably small in comparison to uncertainty estimates for $p_k < p_{k_{th}}$ with similar grid refinement ratio r_k, solution changes between fine and medium grid/time $\varepsilon_{k_{21}}$ and distance $|p_k - p_{kth}|$ from the AR, which results from too small RE error estimate:

$$\delta^*_{RE_{k_1}} = \frac{\varepsilon_{k_{21}}}{r_k^{p_k} - 1} \qquad (1)$$

In the GCI method *FS*=1.25 is much too small and in the C_k method linearly increasing *FS* is also too small. Herein, an improvement to the C_k method is proposed with polynomial increasing *FS* for $p_k > p_{k_{th}}$ based on reflecting the grid/time uncertainty from $p_k < p_{k_{th}}$ for $p_k > p_{k_{th}}$. The improved uncertainty estimates are shown to provide more reasonable intervals of uncertainty for $p_k > p_{k_{th}}$.

II. IMPROVED FS FOR RE ESTIMATED LARGER THAN THEORETICAL ORDER OF ACCURACY

Grid and time convergence studies are conducted with multiple solutions (at least 3) using systematically refined grid sizes or time steps. For monotonic convergence, procedures for estimating grid and time errors are based on RE, which assumes that the error terms are in the form of power series expansion. Results from the numerical solution of the one-dimensional wave and two-dimensional Laplace equation analytical benchmarks show that RE error estimate using Eqn. (1) has the right form/trends, but is only qualitatively not quantitatively accurate due to poorly estimated $p_k < p_{k_{th}}$

$$p_k = \frac{\ln\left(\varepsilon_{k_{32}} / \varepsilon_{k_{21}}\right)}{\ln\left(r_k\right)} \tag{2}$$

except when solutions are very close to the AR. The error estimate can be improved using correction factors, i.e., $\delta^*_{k_1} = C_k \delta^*_{RE_{k_1}}$, which is used to estimate the uncertainty for uncorrected solutions by bounding the error δ^*_k by the sum of the absolute value of the corrected RE error estimate and the absolute value of the amount of the correction with provision for 10% FS in the limit of $C_k = 1$. $FS = U_k \big/ \left|\delta^*_{RE_{k_1}}\right|$ is reflected from $p_k < p_{k_{th}}$ for $p_k > p_{k_{th}}$ [6]. Thus for uncorrected solutions,

$$U_k = FS\left|\delta^*_{RE_{k_1}}\right| = \begin{cases} \left[9.6(1-C_k)^2+1.1\right]\left|\delta^*_{RE_{k_1}}\right| & 0.875 < C_k < 1.125 \\ \left[2\left|1-C_k\right|+1\right]\left|\delta^*_{RE_{k_1}}\right| & 0 < C_k \le 0.875 \quad or \quad C_k \ge 1.125 \end{cases} \tag{3}$$

For corrected solutions, U_{k_C} is based on the absolute value of the amount of the correction:

$$U_{k_C} = \begin{cases} \left[2.4(1-C_k)^2+0.1\right]\left|\delta^*_{RE_{k_1}}\right| & 0.75 < C_k < 1.25 \\ \left[\left|1-C_k\right|\right]\left|\delta^*_{RE_{k_1}}\right| & 0 < C_k \le 0.75 \quad or \quad C_k \ge 1.25 \end{cases} \tag{4}$$

C_k [6] method is equivalent to the GCI, but with a variable *FS* that increases linearly with the distance of solutions increases from the AR, as shown in Fig. 1.

Verification studies have shown that the estimates of U_k and U_{k_C} using Eqns. (3) and (4) are too conservative for $p_k > p_{k_{th}}$, as explained previously. An improved approach is to reflect the uncertainty itself with respect to the distance from the AR instead of reflecting the *FS*. First, $r_k^{p_k}$ in Eqn. (1) is re-expressed based on the definition of C_k:

$$r_k^{p_k} = C_k\left(r_k^{p_{k_{th}}}-1\right)+1 \tag{5}$$

Second, Eqn. (1) is substituted into Eqn. (3) for $0<C_k\le 0.875$ with the use of Eqn. (5), which results in an alternative form of U_k

$$U_k = \left[2(1-C_k)+1\right]\left|\frac{\varepsilon_{k_{21}}}{C_k\left(r_k^{p_{k_{th}}}-1\right)}\right| \qquad 0 < C_k \le 0.875 \tag{6}$$

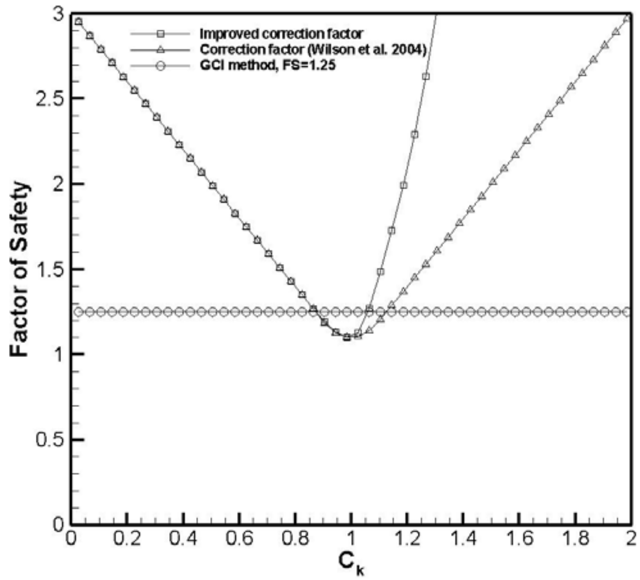

Figure 1. Factors of safety for correction factor and GCI verification methods.

Third, to enforce the same U_k for $1.125 \le C_k < 2$ as the U_k at the same distance to $C_k=1$ within $0 < C_k < 0.875$, C_k in Eqn. (6) is replaced by $2 - C_k$. Thus for the same r_k, $p_{k_{th}}$, and $\varepsilon_{k_{21}}$, Equation (6) becomes:

$$U_k = \left\{ \frac{C_k}{2 - C_k} \left[2\left(C_k - 1 \right) + 1 \right] \right\} \left| \delta^*_{RE_{k_1}} \right| \qquad 1.125 \le C_k < 2 \qquad (7)$$

Additionally, two 3rd order polynomials instead of two quadratic functions as used in [6] are used to generate smoother curves of *FS* for $0.875 < C_k \le 1.0$ and $1.0 < C_k < 1.125$, respectively. The use of higher order polynomials allows not only the *FS* magnitude but also the first order derivative of *FS* with respect to C_k to be continuous at $C_k=0.875$, 1.0, and 1.125, which are used to determine the four unknown coefficients for each polynomial. Following [6], the magnitude and 1st order derivative of *FS* at $C_k=1$ are 1.1 and 0, respectively. Incorporating all of the above revisions the U_k and U_{k_C} are given by:

$$U_k = \begin{cases} \left[2(1-C_k)+1\right] \quad \left|\delta^*_{RE_{k_1}}\right| & 0 < C_k \le 0.875 \\ \left[-25.6(1-C_k)^3 + 12.8(1-C_k)^2 + 1.1\right]\left|\delta^*_{RE_{k_1}}\right| & 0.875 < C_k \le 1.0 \\ \left[-135.8(C_k-1)^3 + 49.4(C_k-1)^2 + 1.1\right]\left|\delta^*_{RE_{k_1}}\right| & 1.0 < C_k < 1.125 \\ \left\{\dfrac{C_k}{2-C_k}\left[2\left(C_k-1\right)+1\right]\right\}\left|\delta^*_{RE_{k_1}}\right| & 1.125 \le C_k < 2 \end{cases} \tag{8}$$

$$U_{k_C} = \begin{cases} (1-C_k)\left|\delta^*_{RE_{k_1}}\right| & 0 < C_k \le 0.75 \\ \left[-3.2(1-C_k)^3 + 3.2(1-C_k)^2 + 0.1\right]\left|\delta^*_{RE_{k_1}}\right| & 0.75 < C_k \le 1.0 \\ \left[-16.98(C_k-1)^3 + 12.35(C_k-1)^2 + 0.1\right]\left|\delta^*_{RE_{k_1}}\right| & 1.0 < C_k < 1.25 \\ \left(\dfrac{C_k^2 + 2C_k - 3}{3-C_k}\right)\left|\delta^*_{RE_{k_1}}\right| & 1.25 \le C_k < 2 \end{cases} \tag{9}$$

Compared to C_k [6], the improved C_k method introduces an additional term $C_k/(2-C_k)$ to compute U_k for $1.125 \le C_k < 2$. When C_k increases, this term increases rapidly from 1 to infinity, which amplifies *FS* when solutions are further away from the AR. The improved C_k method is only applicable for $0<C_k<2$. $C_k=0$ is the border of convergence and divergence such that grid errors/uncertainties are infinite due to infinite $\delta^*_{RE_{k_1}}$ as a result of $p_k=0$, i.e. solution changes for the medium and fine grids are equal to those for the coarse and medium grids. For $C_k>2$, solutions are too far from the AR and also regarded as divergent. Figure 1 compares *FS* predicted by the improved C_k, C_k [6], and GCI methods with a zoomed in view near the AR shown in Fig. 2.

Compared with the C_k [6] method, the improved C_k method is more conservative for $C_k>0.875$ except with the same *FS* at $C_k=1$. The intersection points between the improved C_k and GCI methods depends on value *FS* used in GCI, e.g., for $FS=1.25$ intersection points are C_k= (0.875, 1.06) and (0.75, 1.12) for uncorrected and corrected solutions, respectively. When solutions are between the intersection points, i.e., closer to the AR, the GCI method is more conservative than the improved C_k method. When solutions are outside the intersection points, i.e., further from the AR, the GCI method is less conservative than the improved C_k method.

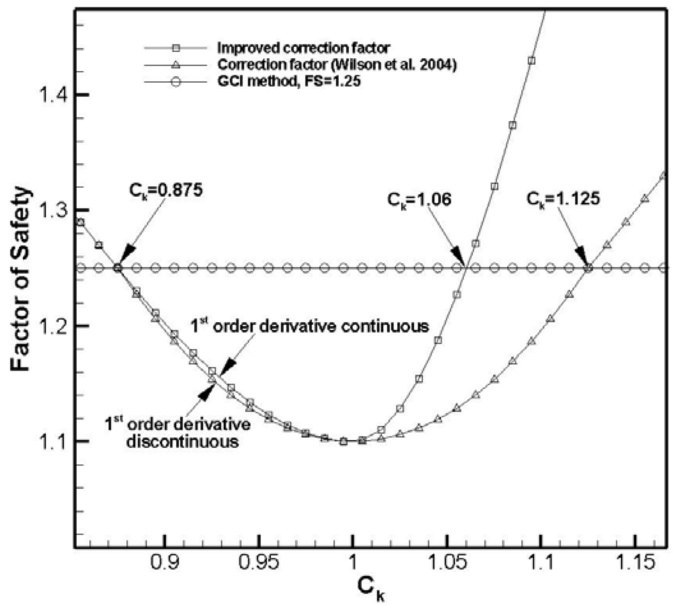

Figure 2. A zoomed in view of factors of safety for correction factor and GCI verification methods.

III. EXAMPLES FOR SHIP HYDRODYNAMICS APPLICATIONS

To demonstrate that the improved C_k method predicts more reasonable intervals of grid uncertainties than C_k [6] and GCI methods for industrial applications, the three methods are applied for a recent study [7] that used computational towing tank procedures for single run curves of resistance and propulsion for the high-speed transom ship Athena barehull with a skeg using the general-purpose solver CFDShip-Iowa-V.4 [8]. Extensive verification (for grid) and validation (not shown herein) studies are conducted by continuously refining the grid from the coarsest grid (grid 7 with 360,528 points; $y_1^+ = 4.26$) to the finest grid (grid 1 with 8.1 million points; $y_1^+ = 1.52$) for the Athena bare hull with skeg with 2 degrees of freedom (pitch and heave) at Froude number (Fr) 0.48. The grids are designed with a systematic grid refinement ratio $r_G = 2^{1/4}$, which allows 9 sets of grids for verification and validation (V&V) with 5 sets with $r_G =$

$2^{1/4}$ (5,6,7; 4,5,6; 3,4,5; 2,3,4; and 1,2,3), 3 sets with $r_G = 2^{1/2}$ (3,5,7; 2,4,6; and 1,3,5), and 1 set with $r_G = 2^{3/4}$ (1,4,7). Figure 3(a) and 3(c) show the solutions with EFD data for the resistance coefficients and ship motions, respectively. Figure 3(b) and 3(d) show the relative solution changes between two successive grids with iterative errors for the resistance coefficients and ship motions, respectively. The coarsest grid 7 is too coarse as its solution is out of the trend shown for the other grid solutions. ε_N shows systematic decreasing for C_{TX}, C_{fX}, and trim with $U_I < \varepsilon_N$ for the coarse grids. ε_N shows oscillatory decreasing for C_{PX} and sinkage, which is caused by the problem of separating the iterative errors U_I and ε_N for the fine grids as they are of the same order of magnitude. Overall U_I is insensitive to the refinement of grids and the average U_I is 0.18%, 0.15%, and 0.2% for C_{TX}, sinkage and trim, respectively. C_{TX} monotonically converges for 6 sets of grids except those with the coarsest grid 7 involved, whereas motions are more difficult to converge. Verification results for monotonic converged solutions are presented in Tables 1 and 2 for the total resistance coefficient and ship motions, respectively. C_G shows large range of oscillations ($0.07 \le C_G \le 2.42$ for C_{TX} and $0.40 \le C_G \le 16.92$ for ship motions) indicating that the solutions are not yet in the AR.

Table 1. Verification study for C_{TX} of Athena bare hull with skeg (*Fr*=0.48). U_G is $\%S_{fine}$; C_{TX} is based on static wetted area; Factor of safety for GCI is 1.25

Grids	*Refinement Ratio*	R_G $\left(\varepsilon_{G_{21}}/\varepsilon_{G_{32}}\right)$	p_G	C_G	U_G (%)		
					Xing and Stern	C_k [6]	*GCI*
2, 4, 6	$\sqrt{2}$	0.63	1.32	0.58	4.90	4.90	3.34
1, 3, 5	$\sqrt{2}$	0.40	2.66	1.51	**3.59**	1.16	0.72
4, 5, 6	$\sqrt[4]{2}$	0.97	0.16	0.07	125.2	125.2	52.7
3, 4, 5	$\sqrt[4]{2}$	0.80	1.27	0.59	7.23	7.23	4.98
2, 3, 4	$\sqrt[4]{2}$	0.60	2.98	1.64	**8.73**	4.27	1.07
1, 2, 3	$\sqrt[4]{2}$	0.50	4.00	2.42	—	1.11	0.58

As shown in Table 1, U_G of C_{TX} for grids (4,5,6) is unreasonable large as it is too far away from the asymptotic range. U_G of C_{TX} for grids (1,2,3) using the C_k [6] is unreasonable small due to the deficiency discussed above. Excluding these two numbers, the average U_G are 2.53%, 4.39%, and 6.11% for the GCI, C_k [6], and improved C_k methods, respectively. For $p_G > p_{G_{th}}$ on grids (2,3,4), the improved C_k method predicts more reasonable U_G (8.73%), which is 2 times the magnitude using C_k [6] method and one order of magnitude larger than that using GCI. When solutions are closer to the AR, the differences between the U_G using the three methods decrease. As shown in Table 2 for trim on grids (1,3,5) where C_G=1.09, U_G is of the same order of magnitude for the three methods. Nonetheless, the improved C_k method is more conservative than GCI and GCI is more conservative than the C_k [6] method, which is consistent with the observation in Fig. 2 for $1.06<C_G\leq 1.125$.

Table 2. Verification study for motions of Athena bare hull with skeg (Fr=0.48). U_G is $\%S_{fine}$; Factor of safety for GCI is 1.25

Parameter	Grids	Refinement Ratio	R_G $\left(\varepsilon_{G_{21}}/\varepsilon_{G_{32}}\right)$	p_G	C_G	U_G (%)		
						Xing and Stern	C_k [6]	*GCI*
Sinkage	1, 3, 5	$\sqrt{2}$	0.31	3.4	2.25	—	1.80	0.64
Sinkage	2, 3, 4	$\sqrt[4]{2}$	0.13	12	16.92	—	1.37	0.05
Trim	1, 3, 5	$\sqrt{2}$	0.48	2.13	1.09	**4.67**	3.88	4.12
Trim	4, 5, 6	$\sqrt[4]{2}$	0.86	0.89	0.40	42.87	42.87	24.42
Trim	2, 3, 4	$\sqrt[4]{2}$	0.53	3.69	2.16	—	8.91	3.35
Trim	1, 2, 3	$\sqrt[4]{2}$	0.53	3.71	2.18	—	4.64	1.73

Overall the improved C_k method provides more reasonable uncertainty estimates for $p_G > p_{G_{th}}$ than the C_k [6] and GCI methods. More accurate and efficient iterative methods (e.g. multi-grid) are needed to speed up the convergence and reduce the U_I especially for the fine grids for improved assessment of grid convergence. Further refinement with $y_1^+ < 1$ may also help reach the AR but requires at least 38 million grid points, which raises issues of code efficiency and available computer resources.

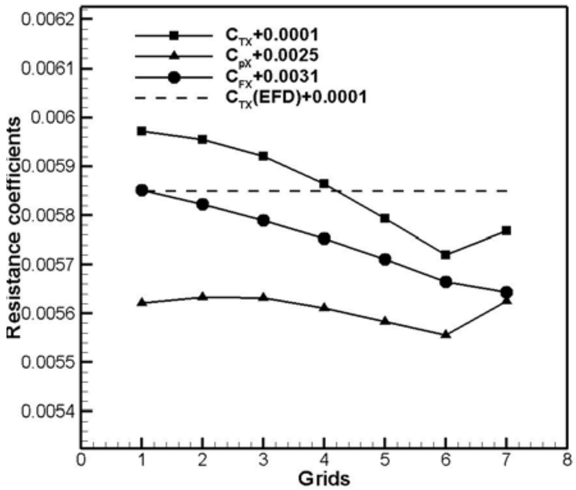
C_TX+0.0001
C_pX+0.0025
C_FX+0.0031
C_TX(EFD)+0.0001
Resistance coefficients
Grids

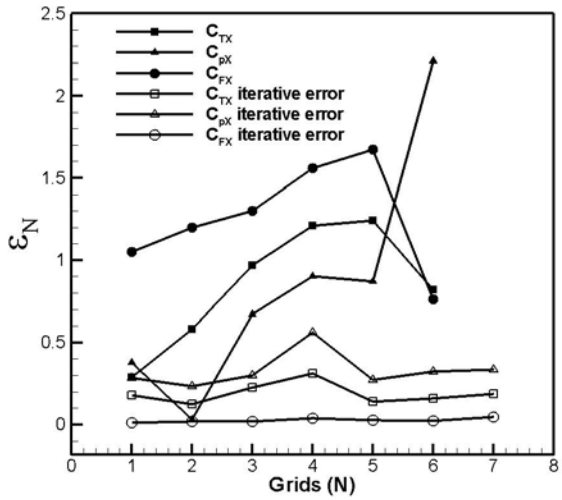
C_TX
C_pX
C_FX
C_TX iterative error
C_pX iterative error
C_FX iterative error
ε_N
Grids (N)

(a) (b)

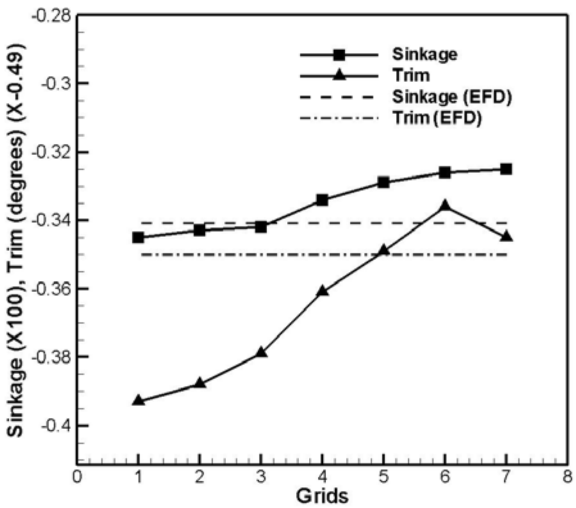

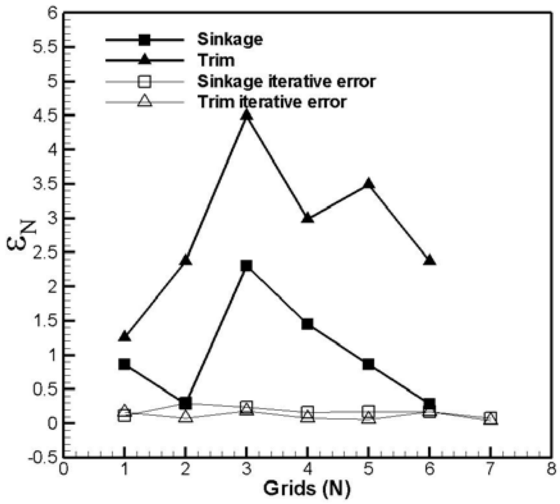

(c) (d)

Figure 3. Verification for resistance and motions for Athena bare hull with skeg (Fr=0.48): (a) resistance coefficients, (b) relative change $\varepsilon_N = |(S_{N-1} - S_N)/S_1| \times 100$ and iterative errors for resistance coefficients, (c) sinkage and trim, (d) relative change ε_N and iterative errors for sinkage and trim.

IV. CONCLUSIONS AND FUTURE WORK

Improved factors of safety for quantitative estimates for grid and time convergence uncertainties for CFD solutions are proposed for situations when Richardson extrapolation estimated order of accuracy p_k is larger than the theoretical order of accuracy $p_{k_{th}}$. The improved uncertainty estimates are shown to provide more reasonable intervals of uncertainty for $p_k > p_{k_{th}}$ and 1<C_k<2.

Since numerical solutions of the analytical benchmarks conducted so far approach the AR with $p_k < p_{k_{th}}$, it is desirable to validate current verification procedures using more advanced numerical benchmarks for complex flows such as backward-facing step flow as the solutions will likely approach the AR similarly as industrial applications, i.e., with oscillatory 1-C_k. The more advanced numerical benchmarks can also be used to validate the validation procedures.

References

[1] Roache, P.J., 1998, "Verification and Validation in Computational Science and Engineering," Hermosa publishers, Albuquerque, NM.

[2] Roache, P., 2003, "Errors Bars for CFD," AIAA 2003-408 41st Aerospace Sciences Meeting, Reno, Nevada, 6-9 January.

[3] ASME, J. Fluids Engineering, http://journaltool.asme.org/Content/AuthorResources.cfm.

[4] Cosner, R.R., Oberkampf, W.L., Rumsey, C.L., Rahaim, C.P., and Shih, T. I-P, 2006, "AIAA Committee on Standards for CFD: Status and Plans," AIAA-2006-889, 44th Aerospace Sciences Meeting, Reno, Nevada, 9-12 January.

[5] Stern, F., Wilson, R.V., Coleman, H., and Paterson, E., 2001, "Comprehensive Approach to Verification and Validation of CFD Simulations-Part 1: Methodology and Procedures," ASME J. Fluids Eng., **123**, pp. 793-802.

[6] Wilson, R. Shao, J., and Stern, F., 2004, "Discussion: "Criticisms of the "Correction Factor" Verification Method" (Roache, P., 2003, ASME J. Fluids Eng., **125**, pp. 732-733)," *ASME Journal of Fluids Engineering*, **126**, pp. 704-706.

[7] Xing, T., Carrica, P., Stern, F., 2008, "Computational Towing Tank Procedures for Single Run Curves of Resistance and Propulsion," accepted, ASME J. of Fluids Engineering.

[8] Carrica, P.M., Wilson, R.V., and Stern, F., 2007, "An Unsteady Single-phase Level Set Method for Viscous Free Surface Flows," Int. J. Numer. Meth. Fluids, **53** (2), pp. 229-256.